# Remote sensing of clear sky turbulence using Doppler lidar. Numerical simulation

**V.A. Banakh, Ch. Werner,* and I.N. Smalikho**

*Institute of Atmospheric Optics,*
*Siberian Branch of the Russian Academy of Sciences, Tomsk, Russia*
** Institute of Atmospheric Physics, Wessling, Germany*

Received June 20, 2001

Based on numerical simulations a possibility of sensing clear sky turbulence with an airborne coherent Doppler lidar is analyzed. It is shown that the accuracy of estimating the turbulence level from lidar data depends on the turbulence intensity, signal-to-noise ratio, and on the number of sounding pulses. The conditions are determined under which the detection is possible of clear sky turbulence areas using a coherent Doppler lidar.

## Introduction

Basic causes of the clear sky turbulence in the free atmosphere are temperature and the wind velocity gradients formed due to interaction of air masses with different characteristics in the regions near atmospheric fronts and altitude frontal zones, as well as the loss of wave stability in the temperature inversion layers, at the tropopause and near other dividing surfaces in the atmosphere, deformation of air currents by mountain obstacles and the formation of wave perturbations at the slopes of mountains.[1] According to data of airborne measurements,[1] in the upper troposphere (at altitudes of 6–10 km) and in the lower stratosphere (up to ~ 25 km) the turbulence with the recurrence period up to 25% can be observed in the broken (with typical horizontal size of separate parts ~ 10 km) and continuous zones, which are transported by the mean flow. In this case the vertical size of the turbulent zones is 1 km.

The areas of increased turbulence under clear sky conditions are dangerous for aircrafts, and to improve the flight safety early detection of such areas on the aircraft flight routes is necessary. For these purposes it is promising to use Doppler lidars. At present the projects are being realized aimed at creating such lidars and at developing the methods of detecting the areas of intense turbulence. Thus Ref. 2 shows the results of first experiments on measuring the dissipation rate of turbulent energy along the aircraft flight using an on-board Doppler lidar.

In this paper, with the use of numerical simulation of a lidar return of an airborne Doppler lidar a possibility is studied of determining the level of turbulent intensity in clear sky from the estimates of the lidar return power spectral width.

## 1. Model of turbulence

The measurements of spectral densities of fluctuations of horizontal (longitudinal) wind velocity component

$$S_u(\kappa) = (2\pi)^{-1} \int_{-\infty}^{+\infty} \mathrm{d}r\, B_u(r)\, \mathrm{e}^{-j\kappa r}\,, \qquad (1)$$

where $B_u(r) = \langle U(r_0 + r)\, U(r_0)\rangle$ is the correlation function, $U$ is the wind velocity fluctuations, have shown[1] that at high spatial frequencies $\kappa$ $10^{-3}$ m$^{-1}$ (up to the boundary of viscous turbulence interval) the density spectrum fits the Kolmogorov–Obukhov law ($S_u(\kappa) \sim \kappa^{-5/3}$), and at low frequencies (outside the limits of the inflow of turbulent energy) the exponent $\nu$ in the power-law relation of spectrum to the spatial frequency ($S_u(\kappa) \sim \kappa^{\nu}$) differs from $\langle -5/3 \rangle$ and, according to different data the exponent varies from $\nu = -2.2$ to $\nu = -3.1$ (on the average, $\nu \approx -2.7$).

The two portions of the spectrum do exist because in the upper troposphere and stratosphere there are, as a rule, conditions of stable temperature stratification. Therefore, the transfer of wind disturbances energy from large-scale vortices to smaller ones is, first, accompanied by the consuming kinetic energy of motion to overcome the Archimedean forces (a high percentage of potential energy of turbulence converts into the potential energy of stratification) and only then in the region of scales corresponding to inertial interval, the process of energy transfer begins to proceed without losses at a constant rate, being equal to the rate of turbulence energy conversion into the heat energy.[1]

The degree of danger from the clear sky turbulence to the aircraft flight stability can be assessed using the four-point scale: weak ($b_1$), moderate ($b_2$), strong ($b_3$), and very strong or storm ($b_4$). Based on the data from Ref. 1 for the spectrum $S_u(\kappa)$ at $\kappa = 2 \cdot 10^{-3}$ m$^{-1}$ and taking into account the fact that at $\kappa \ge 10^{-3}$ m$^{-1}$

$$S_u(\kappa) = 0.25\varepsilon^{2/3}\, \kappa^{-5/3}, \qquad (2)$$

where $\varepsilon$ is the rate of dissipation of turbulent energy, we calculated the values of $\varepsilon$ corresponding to the levels of these four-point scale. The results are given in Table 1.

0235-6880/01/10 856-08 $02.00 

**Table 1**

| Intensity of turbulence | Dissipation rate of the turbulence energy ε, $m^2/s^3$ |
|---|---|
| $b_1$ | $10^{-3} - 5 \cdot 10^{-3}$ |
| $b_2$ | $5 \cdot 10^{-3} - 1.5 \cdot 10^{-2}$ |
| $b_3$ | $1.5 \cdot 10^{-2} - 4.5 \cdot 10^{-2}$ |
| $b_4$ | $\geq 4.5 \cdot 10^{-2}$ |

The airplane responds not to any turbulent gusts but only to the disturbances from a relatively narrow range of turbulence spectrum. In particular, the vortex structures of the size from 10–20 m up to 3–4 km (for heavy airplanes – 6 or 7 km) produce an effect on the airplane motion at subsonic speeds.[1] The estimates of turbulence energy $\int_{\kappa_1}^{\kappa_2} d\kappa S_u(\kappa)$ made by the authors in the frequency range from $\kappa_1 = 3 \cdot 10^{-4}\ m^{-1}$ to $\kappa_2 = 3 \cdot 10^{-1}\ m^{-1}$ based on the assumption that the spectrum is described by formula (2) with $\kappa \geq 10^{-3}\ m^{-1}$ and $S_u(\kappa) = A\kappa^{-2.7}$ for $\kappa < 10^{-3}\ m^{-1}$ where, according to the data from Ref. 1, $A \approx 10^{-6}\ (m^3/s) \cdot m^{-2.7}$ and using only the formula (2) for the entire range $[\kappa_1, \kappa_2]$ indicated that both types of calculations gave close results for the turbulence energy practically for all the values of ε cited in Table 1. Therefore later on we shall use the spectral model (2) for the entire frequency range.

## 2. Algorithms of numerical simulation of lidar return and assessment of turbulence level

Let us assume that a coherent Doppler lidar is installed on board an aircraft and sensing of turbulence is performed along the direction of the aircraft flight. The lidar receiving system records a lidar return due to scattering of sounding pulse on aerosol particles, entrained by the wind $z(mT_s)$, as a function of time $t = t_0 + mT_s$, where $t_0$ is the time of the start of measurements, $T_s = B^{-1}$ is the frequency of data reading, $B$ is the receiver's transmission band, $m = 0, 1, 2, \ldots$ . From $z(mT_s)$ the data are extracted on the turbulence in the volume sounded at a distance $ct_0/2$, where $c$ is the speed of light. The turbulence can also be estimated from a series of lidar returns $z(mT_s)$ from several sounding pulses with the use of a corresponding procedure of data storage.

According to Ref. 3 and expression for a normalized complex signal, the function $z(mT_s)$ takes the form:

$$z(mT_s) = \left( \frac{SNR}{2\sqrt{\pi}} \frac{\Delta P}{P} \right)^{1/2} \sum_{k=0}^{n_L} a(k + ml) \times \exp\left\{ -\frac{1}{2} \left(\frac{\Delta P}{P}\right)^2 \left( \frac{n_L}{2} - k \right)^2 - j\, \frac{4\pi}{\lambda}\, mT_s\, V_r\, (\Delta P(k + ml)) \right\} + \frac{1}{\sqrt{2}}\, n_m, \quad (3)$$

where $SNR$ is the signal-to-noise ratio, $n_L = [4\sqrt{2}P/\Delta P]$ is the number of layers, into which the volume sounded is divided; $\Delta P$ is the thickness of a separate layer; $P = \sigma_p c/2$; $\sigma_p$ is the duration of a sounding pulse; $l = [cT_s/(2\Delta P)]$; $a(k)$ and $n_m$ are independent complex random values with the zero mean and Gaussian distribution of the probability density (variances of the real and imaginary parts are equal to unity); λ is the wavelength of sounding radiation. The radial (along the direction of sounding) speed component $V_r(z)$ in Eq. (3) is simulated in the spectral range using Eq. (2) for the fluctuation power spectra of the wind velocity. The values of $SNR$ in Eq. (3) for the aircraft sounding paths were calculated by the formula[3,4]:

$$SNR = \frac{\eta_q\, U_p\, c\beta_\pi}{h\nu B} \frac{e^{-2\alpha_a R}}{12\pi^2} \left( \frac{\lambda}{a_t} \right)^2 \frac{1}{1 + \left( \frac{3}{2\pi} \frac{\lambda R}{a_t^2} \right)}, \quad (4)$$

assuming homogeneity of the light-scattering characteristics of the medium (along a horizontal path) and that turbulent fluctuations of the refractive index of the air can be neglected. In the expression (4) $\eta_q$ is the detector quantum efficiency, $U_p$ is the sounding pulse power, $h\nu$ is the photocurrent power, $\beta_\pi$ is the backscattering coefficient, $\alpha_a$ is the extinction coefficient, $R$ is the sounding path length; $a_t$ is the transmitting aperture radius.

Figure 1 shows the $SNR$ as functions of the backscattering coefficient $\beta_\pi$ at 5–20 km altitudes,[5,6] and the sounding pulse power $U_p$ for lidar with $\lambda = 2.09$ μm, $a_t = 10$ cm, $\eta_q = 0.4$, $\beta = 50$ MHz, and $R = 10$ km. It is clear that the values of $SNR$, depending on $\beta_\pi$ and $U_p$, can vary within five orders of magnitude: from $\sim 10^{-4}$ to $\sim 10$.

An important condition in lidar detection of turbulence at a definite distance along a trajectory of aircraft motion is the promptness of obtaining necessary information. In this regard the most suitable method is the evaluation of turbulence intensity from the power spectrum width of a Doppler-lidar return, determined by random, due to the turbulence, scatter in speeds of scattering particles in a volume sounded.

For the $i$th sounding pulse normalized to the square root of the mean noise power and demodulated taking into account the frequencies of the reference and sounding beams and the Doppler frequency shift of a complex signal $z_i(mT_s)$ due to the aircraft motion, one can obtain the estimate of the spectral density $\hat{W}_i(k/T)$ using FFT:

$$\hat{W}_i\left(\frac{k}{T}\right) = \frac{1}{T} \left| T_s \sum_{m=0}^{M-1} z_i(mT_s) \exp\left( -2\pi j\, \frac{mk}{M} \right) \right|^2, \quad (5)$$

where $T = MT_s$ is the time of measurement, $k = 0, 1, \ldots, M - 1$. At a sufficiently high pulse-repetition rate $f_p$ it is possible to obtain the estimate of the mean spectrum $n^{-1}\sum_{i=1}^{n} \hat{W}_i(k/T)$ with a high degree of accuracy, where $n$ is the number of pulses selected so that the random distribution of wind velocity over the sounding volume can be considered to be "frozen" and at a given time $n/f_p$ an essential shift of the sounding volume is not observed due to the aircraft motion. Using the expression from Ref. 3 for $z(mT_s)$ and Eq. (5), after passing in equation (5) from summation to integration, with the account of the condition $T_s \ll \sigma_p \ll T$, and averaging over the ensemble for all parameters, except for the velocity $V_r(z)$, for the average spectrum $\overline{W(f)} = \overline{\hat{W}(f)} - W_N$, we obtain

$$\overline{W(f)} = SNR \frac{4}{cT} \int_{-\infty}^{+\infty} dz \int_{-T/2}^{T/2} dt \times$$

$$\times \exp\left\{-\frac{[t + (R - z)2/c]^2}{\sigma_p^2} - \sigma_p^2(2\pi)^2 [f - \frac{2}{\lambda} V_r(z)]^2\right\}, \quad (6)$$

where

$$SNR = \int_{-\infty}^{+\infty} df\, \overline{W(f)}; \quad (7)$$

$W_N = T_s$ is the mean noise spectral component and here $k/T \to f$.

Taking into account the Doppler ratio $V = f\lambda/2$, the lidar estimate of radial wind velocity $V_D$ in the sounding volume is determined as the first moment:

$$V_D = \frac{\lambda}{2} \frac{1}{SNR} \int_{-\infty}^{+\infty} dff\, \overline{W(f)}\ . \quad (8)$$

After substituting Eq. (6) into Eq. (8) we have

$$V_D = \int_{-\infty}^{+\infty} dz\, Q_s(z) V_r(z)\ , \quad (9)$$

where

$$Q_s(z) = \frac{1}{cT}\left[\operatorname{erf}\left(\frac{2}{c\sigma_p}(R - z) + \frac{T}{2\sigma_p}\right) - \operatorname{erf}\left(\frac{2}{c\sigma_p}(R - z) - \frac{T}{2\sigma_p}\right)\right] \quad (10)$$

is the function characterizing the visibility and longitudinal size of the sounding volume,[3] erf $(x)$ is the probability interval.

Now we determine the square of the Doppler spectral broadening $\Delta V_D^2$ (in velocity units) as the second central moment:

$$\Delta V_D^2 = SNR^{-1} \int_{-\infty}^{+\infty} df\, (f\lambda/2 - V_D)^2\, \overline{W(f)}\ . \quad (11)$$

From Eqs. (6) and (11) we obtain

$$\Delta V_D^2 = \left(\frac{\lambda}{2}\right)^2 \frac{1}{8\pi^2 \sigma_p^2} + \int_{-\infty}^{+\infty} dz\, Q_s(z)[V_r(z) - V_D]^2. \quad (12)$$

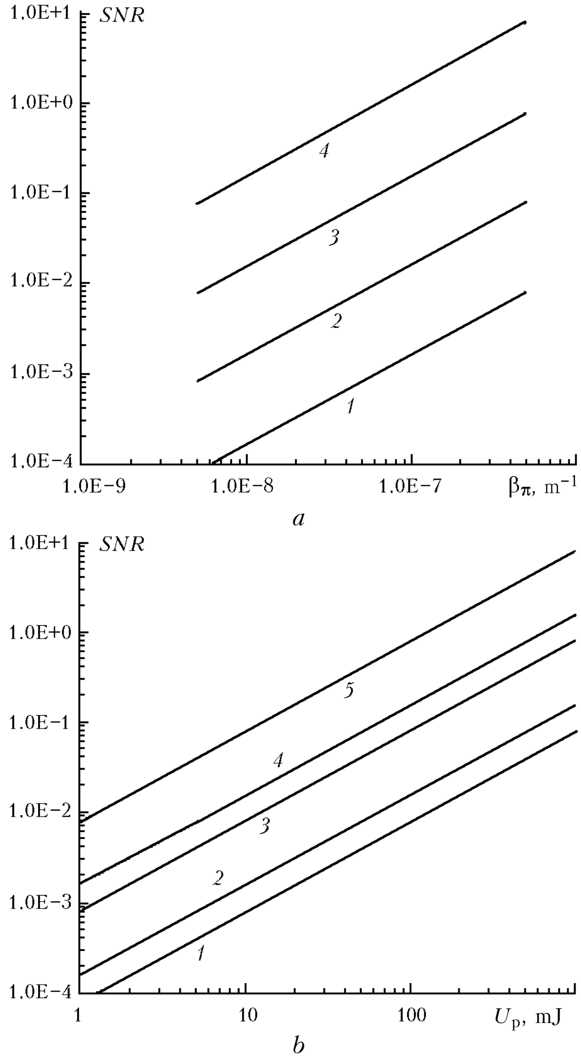


**Fig. 1.** The dependence of the signal-to-noise ratio on the backscattering coefficient $\beta_\pi$ (*a*) and the sounding pulse power $U_p$ (*b*); (*a*) $U_p$ = 1 (*1*); 10 (*2*); 100 (*3*), and 1000 mJ (*4*); (*b*) $\beta_\pi = 5\cdot10^{-9}$ (*1*); $10^{-8}$ (*2*); $5\cdot10^{-8}$ (*3*); $10^{-7}$ (*4*), and $5\cdot10^{-7}$ m$^{-1}$ (*5*).

For the mean value of the square of the Doppler spectral broadening $\sigma_s^2 = \langle\Delta V_D^2\rangle$, where the brackets denote averaging over the ensemble of wind velocity, from Eq. (12) taking into account the model chosen for the turbulence [formula (2)] we have

$$\sigma_s^2 = \sigma_{sp}^2 + \sigma_{st}^2\ , \quad (13)$$

where

$$\sigma_{sp}^2 = \left(\frac{\lambda}{2}\right)^2 \frac{1}{8\pi\sigma_p^2} \quad (14)$$

is the square of the Doppler spectral broadening in the absence of turbulence,

$$\sigma_{st}^2 = 0.5\varepsilon^{2/3} \int_0^{\infty} d\kappa\kappa^{-5/3}\, [1 - H(\kappa)] \quad (15)$$

is the component due to the contribution of turbulence to the Doppler spectral broadening,

$$H(\kappa) = \exp\left\{-\frac{1}{2}(\sigma_p c/2)^2\kappa^2\right\}\text{sinc}^2\left(\frac{1}{2}\kappa\frac{cT}{2}\right) \quad (16)$$

is the transmission function of the low-frequency filter, $\text{sinc}(x) = \sin(x)/x$.

The integral in expression (15) can be calculated analytically for two asymptotic cases $\sigma_p \gg T$ and $\sigma_p \ll T$. When the pulse duration far exceeds the measurement time of the unsmoothed spectrum $\hat{W}_i(f)$ ($\sigma_p \gg T$)

$$\sigma_{st}^2 = c_1\varepsilon^{2/3}(\sigma_p c/2)^{2/3}, \quad (17)$$

where $c_1 = 0.5\,\Gamma(1/3)2^{-4/3} \approx 0.53$. For the case of $T \gg \sigma_p$ we obtain, from Eq. (15), being of prime practical interest, that

$$\sigma_{st}^2 = c_2\varepsilon^{2/3}(Tc/2)^{2/3}, \quad (18)$$

where $c_2 = 0.5\,\Gamma(1/3)27/80 \approx 0.45$.

The values of the Doppler spectral broadening $\sigma_s$, calculated by the formula (13) and corresponding to different turbulent levels from Table 1, are given in Table 2. The calculations have been made using the following parameters: $\lambda = 2.09$ µm, $\sigma_p = 1$ µs, $T = 20.48$ µs ($T = T_s M$, $T_s = 20$ ns, $M = 1024$). In this case the longitudinal size of the sounding volume $\Delta z = Q_s^{-1}(R)$ (Ref. 3) is about 3 km.

**Table 2**

| Dissipation rate of the turbulence energy ε, $m^2/s^3$ (Intensity of turbulence) | | Width of the Doppler spectrum, m/s |
|---|---|---|
| $10^{-3} - 5\cdot10^{-3}$ | ($b_1$) | 0.97 – 1.65 |
| $5\cdot10^{-3} - 1.5\cdot10^{-2}$ | ($b_2$) | 1.65 – 2.39 |
| $1.5\cdot10^{-2} - 4.5\cdot10^{-2}$ | ($b_3$) | 2.39 – 3.45 |
| $\geq 4.5\cdot10^{-2}$ | ($b_4$) | ≥ 3.45 |

In the absence of turbulence ($\varepsilon = 0$) $\sigma_s = \sigma_{sp} = \lambda/(\sqrt{2}\,4\pi\sigma_p) \approx 0.1$ m/s, i.e., it is comparable with the spectral resolution in the velocity $\Delta V = \lambda/(2T) \approx 0.05$ m/s. With the increase in the intensity of turbulence, the spectral broadening increases up to 3.45 m/s and more.

According to data given in Table 2, for the selected parameters $\sigma_p$ and $T$ at $\sigma_s < 0.97$ m/s the turbulence will not have a pronounced effect on the aircraft.

The longitudinal size of the sounded volume is 3 km at $T \approx 20$ µs and it is commensurable with the upper limit of scales of wind turbulent disturbances affecting the flight of a subsonic aircraft. It is evident that even at statistical inhomogeneity of wind turbulence the spectral broadening estimated by the formula (11) will fluctuate greatly in passing from one sounded volume to another since $V_r(z)$ is a random function and the greatest scale of wind disturbances is much larger than the size of a volume sounded.

To obtain a stable estimate of $\sigma_s$, it is essential to average over the ensemble of realizations of $\Delta V_D^2$ corresponding to nonoverlaping volumes sounded. Therefore, the net longitudinal size of the volume sounded, $N\Delta z$, where $N$ is the number of realizations, can far exceed the sounding path length $R$. However, if an airborne lidar is intended for provisional information on the presence of the areas with intense turbulence at a definite distance from the aircraft, then the averaging of the values of $\Delta V_D^2$ loses its meaning. In this case we propose to proceed as follows. The value of $\Delta V_D$ is measured (from a sounded volume spaced from the aircraft at $R = 10$ km). Then, depending on the range of the Doppler broadening values in what $\Delta V_D$ falls, the dissipation rate of turbulent energy is determined and, accordingly, the force of the bumpy air, which (if the estimate of $\Delta V_D$ is true) affects the aircraft after it covers the distance $R$. Thus, Table 2 may be used to determine the "running" level of turbulence (bumpy air force) by the value $\Delta V_D$ measured in routine mode.

The results of numerical simulation and estimation of the Doppler broadening by formula (11) have shown that such a procedure of extracting information on the turbulence is acceptable only at high signal-to-noise ratios ($SNR$). At $SNR < 1$, as a rule, the estimated value is far in excess even at spectral smoothing by a selected spectral window and at the corresponding account of the mean noise level $W_N$. An attempt to average the spectra obtained from different sounding pulses reduces somewhat the requirements to $SNR$, but, as the experience shows, the realization of this approach, taking into account the data in Fig. 1, is impossible.

To assess the Doppler broadening $\hat{\sigma}_s$ from $\tilde{W}(k) = n^{-1}\sum_{i=1}^{n}\hat{W}_i(k/T)$, we used the procedure of fitting the $\tilde{W}(k)$ to a certain model spectrum

$$W_G(k) = \hat{SNR}\,\frac{\lambda}{2}\frac{1}{\sqrt{2\pi}\,\hat{\sigma}_s}\times$$

$$\times\exp\left\{-\frac{1}{2}\left(\frac{\Delta V}{\hat{\sigma}_s}\right)^2\left(k-\frac{\hat{V}_D}{\Delta V}\right)^2\right\} + T_s \quad (19)$$

using the least squares method. In Eq. (19) $\hat{SNR}$ and $\hat{V}_D$ are the estimates of $SNR$ and the radial wind velocity averaged by the volume sounded, $\Delta V = \lambda/(2T)$ is the spectral resolution in the wind speed, $T = T_s M$. Based on determination of the discrepancy minimum using the least squares method

$$\rho\hat{\sigma}_s = \sum_{k_{max}-M/4}^{k_{max}+M/4}[\tilde{W}(k) - W_G(k)]^2 \quad (20)$$

the unknown quantity $\hat{\sigma}_s$ was determined, where $k_{max}$ is the number of the spectral channel, in which $\tilde{W}(k)$ has maximum. The value of $\widehat{SNR}$ in Eq. (19) can be found with a high degree of accuracy using a large bulk of data measured before the moment of turbulence sensing in a considered volume (if the scattering medium is statistically homogeneous). The estimate of wind velocity $\hat{V}_D$ was found by the iteration method. For this purpose, first the value $\Delta V k_{max}$ was assigned to $\hat{V}_D$. Then, according to the median in the selected range $[k_{max} - k_1, k_{max} + k_1]$, where $k_1 = [\hat{\sigma}_s/\Delta V]$, $\hat{\sigma}_{s1}$ is the estimate of spectral broadening with the use of Eqs. (19) and (20) at $\hat{V}_D = \Delta V k_{max}$, we determined $\hat{V}_D$, which finally was used in Eqs. (19) and (20) to find $\hat{\sigma}_s$.

The spectral component containing the information on the turbulence will differ from the Gaussian distribution (the first term in the right-hand side of Eq. (19) even at very sharp ($n \gg 1$) averaging of the signal and noise fluctuations. The reason is that no averaging happens by the wind perturbations with the scales compared with the longitudinal size of the volume sounded. Nevertheless, the numerical experiments have shown that the calculation by formula (12) $\hat{\sigma}_s = \Delta V_D$ and the evaluation of $\hat{\sigma}_s$ with the use of Eqs. (19) and (20) at $SNR \gg 1$ and $n \gg 1$ give the results, which are in close agreement (on the average, the difference is no more than 10%).

## 3. Results of numerical simulation

At numerical simulation of the lidar return $z(mT_s)$ we used the following parameters: $\lambda = 2.09$ μm, $T_s = 20$ ns, $M = 1024$, and $\sigma_p = 1$ μs. The $SNR$ values varied from 10 to $10^{-3}$. The values of the dissipation rate ε were selected to meet the limits of turbulence levels $b_i$ (see Table 1), i.e., $\varepsilon = 10^{-3}$; $5 \cdot 10^{-3}$; $1.5 \cdot 10^{-2}$, and $4.5 \cdot 10^{-2}$ m²/s³. From simulated data the Doppler spectra of $\tilde{W}(k)$ were calculated at different $n$, but at a constant distribution of speed $V_r(z)$ along the sounding path. The number $n$ varied from 1 to 100. We used the moving smoothing of spectra using the window of 7 spectral channels ($7\Delta V \approx 0.35$ m/s).

Figure 2 shows 4 examples of simulating the Doppler spectra in the absence of noise ($SNR^{-1} = 0$) at different levels of turbulence. Here and further the argument of spectra is the velocity $V = (\lambda/2)f$. All the spectra were obtained from a single sounding pulse ($n = 1$).

Figure 3 shows examples of simulating the Doppler spectra corresponding at different $n = 1$ (*1*), $n = 10$ (*2*), $n = 100$ (*3*) to the same random realization of $V_r(z)$ when $SNR = 0.1$ (*a*) and $SNR = 0.01$ (*b*). Here the designation $V' = V - V_D$ is used. It is evident that at $SNR = 0.01$ and $n = 1$ the signal peak is fully immersed in the noises and it is impossible to assess its width. However, when averaging over 100 realizations it is possible to assess the spectral broadening.

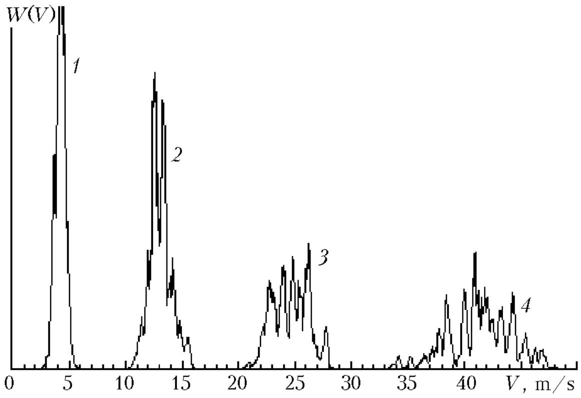


**Fig. 2.** Examples of simulation of the Doppler spectra $W(V)$ at $SNR^{-1} = 0$ and $\varepsilon = 10^{-3}$ (*1*), $5\cdot10^{-3}$ (*2*), $1.5\cdot10^{-2}$ (*3*), and $4.5\cdot10^{-2}$ m²/s³ (*4*).

In Fig. 4 for $n = 1$ examples are shown of the numerical simulation of spectra (solid curves) at $SNR = 0.1$ and the results of fitting by the method of least squares to the Gaussian spectrum (19) (dashed curve) at different levels of the turbulence intensity.

To assess the reliability of detecting the areas of clear sky turbulence based on the Doppler spectrum $\Delta V_D$ measured in a routine mode depending on the number of pulses (accumulation of data) at different $n$, the value of

$$\langle\langle\varepsilon_W^2\rangle\rangle^{1/2} = \langle\langle(\Delta V_D - \hat{\sigma}_s)^2\rangle\rangle^{1/2}$$

was calculated characterizing in a statistical sense the difference of $\Delta V_D$ from the mean Doppler broadening (13). To calculate the error of $\langle\langle\varepsilon_W^2\rangle\rangle^{1/2}$, a sample of 1000 random realizations was used. The calculated results are given in Table 3. According to the data from Tables 1–3 the relative error of estimating the Doppler broadening $\langle\langle\varepsilon_W^2\rangle\rangle^{1/2}/\sigma_s$ by the value $\Delta V_D$ (12) and, respectively, the error of determination of the turbulence level in the areas of clear sky turbulence dangerous for aircraft is 25% at $n = 1$ and $SNR = 1$. It is 50% at $n = 1$ and $SNR = 0.1$; 37% at $n = 100$ and $SNR = 0.01$ practically at any values of the dissipation rate of turbulent energy ε given in Table 3.

**Table 3**

| Dissipation rate of the turbulence energy ε, m²/s³ | $n = 1$, $SNR = 1$ | $n = 1$, $SNR = 0.1$ | $n = 100$, $SNR = 0.01$ |
|---|---|---|---|
| $10^{-3}$ | 0.25 | 0.48 | 0.36 |
| $5 \cdot 10^{-3}$ | 0.39 | 0.86 | 0.61 |
| $1.5 \cdot 10^{-2}$ | 0.60 | 1.24 | 0.92 |
| $4.5 \cdot 10^{-3}$ | 0.76 | 1.51 | 1.21 |

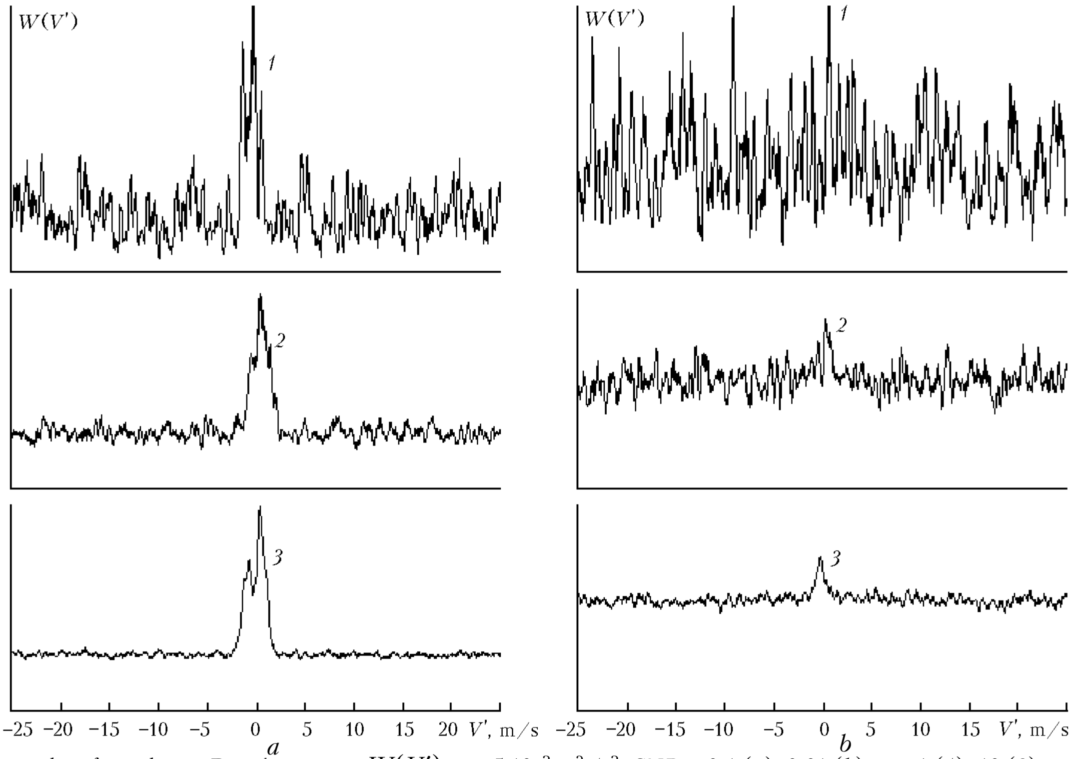


**Fig. 3.** Examples of simulating Doppler spectra $W(V')$; $\varepsilon = 5{\cdot}10^{-3}$ m$^2$/s$^3$, $SNR = 0.1$ (*a*), 0.01 (*b*), $n = 1$ (*1*); 10 (*2*), and 100 (*3*).

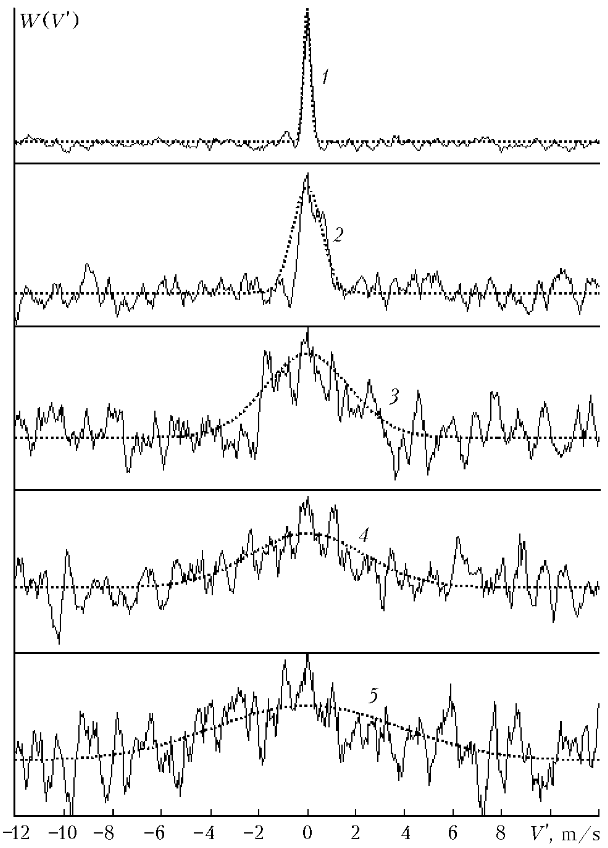


**Fig. 4.** Examples of simulating Doppler spectra $W(V')$ (solid curves) and the results of spectra fitting to the Gaussian dependence on the velocity (dashed curves) at $SNR = 0.1$ and $n = 1$; $\varepsilon = 0$ (*1*); $10^{-3}$ (*2*); $5{\cdot}10^{-3}$ (*3*); $1.2{\cdot}10^{-2}$ (*4*) and $4.5{\cdot}10^{-2}$ m$^2$/s$^3$ (*5*).

Figure 5 shows histograms of the distribution of absolute error $\varepsilon_W = \Delta V_D - \hat{\sigma}_s$, calculated from the simulated data, within the intervals $[\varepsilon_W - \Delta\varepsilon_W/2, \varepsilon_W + \Delta\varepsilon_W/2]$, where $\Delta\varepsilon_W = 0.2$ m/s and $N_e$ is the number of "hits" of the error values $\varepsilon_W$ into one or another interval.

From the results given in Table 3 and Fig. 5 it follows that the absolute error of estimating the Doppler broadening grows with increasing force of turbulence. A decrease in the *SNR* also results in an increase of the errors (both absolute and relative). The results of numerical experiments show that $\hat{\sigma}_s$ at $SNR \le 0.01$ is estimated from a single sounding pulse ($n = 1$) with a very large error, and in this case it is impossible to determine the turbulence level. However, as follows from Table 3 and Fig. 5*c*, at $SNR = 0.01$ the averaging over one hundred Doppler spectra ($n = 100$) can give an acceptable result. The numerical simulation of spectra at $n = 100$ and $SNR = 10^{-3}$ shows that in this case the error of estimating the value $\hat{\sigma}_s$ is too large. Hence, at such a low level of lidar return a larger number of averaging should be made.

At a strong sidewind during the aircraft flight toward the detected dangerous turbulent area the radial velocity $V_r(z)$ can change, and the turbulence intensity inside the sounded volume can change as well. However, as the results of numerical experiments show, the value of the relative fluctuations of the Doppler broadening $E_{\Delta V} = [\langle(\Delta V_D/\sigma_{st} - 1)^2\rangle]^{1/2}$, determined by the turbulent inhomogeneities with scales exceeding the size of sounding volume, equals about 0.3 at any values of $\varepsilon$ from Table 1.

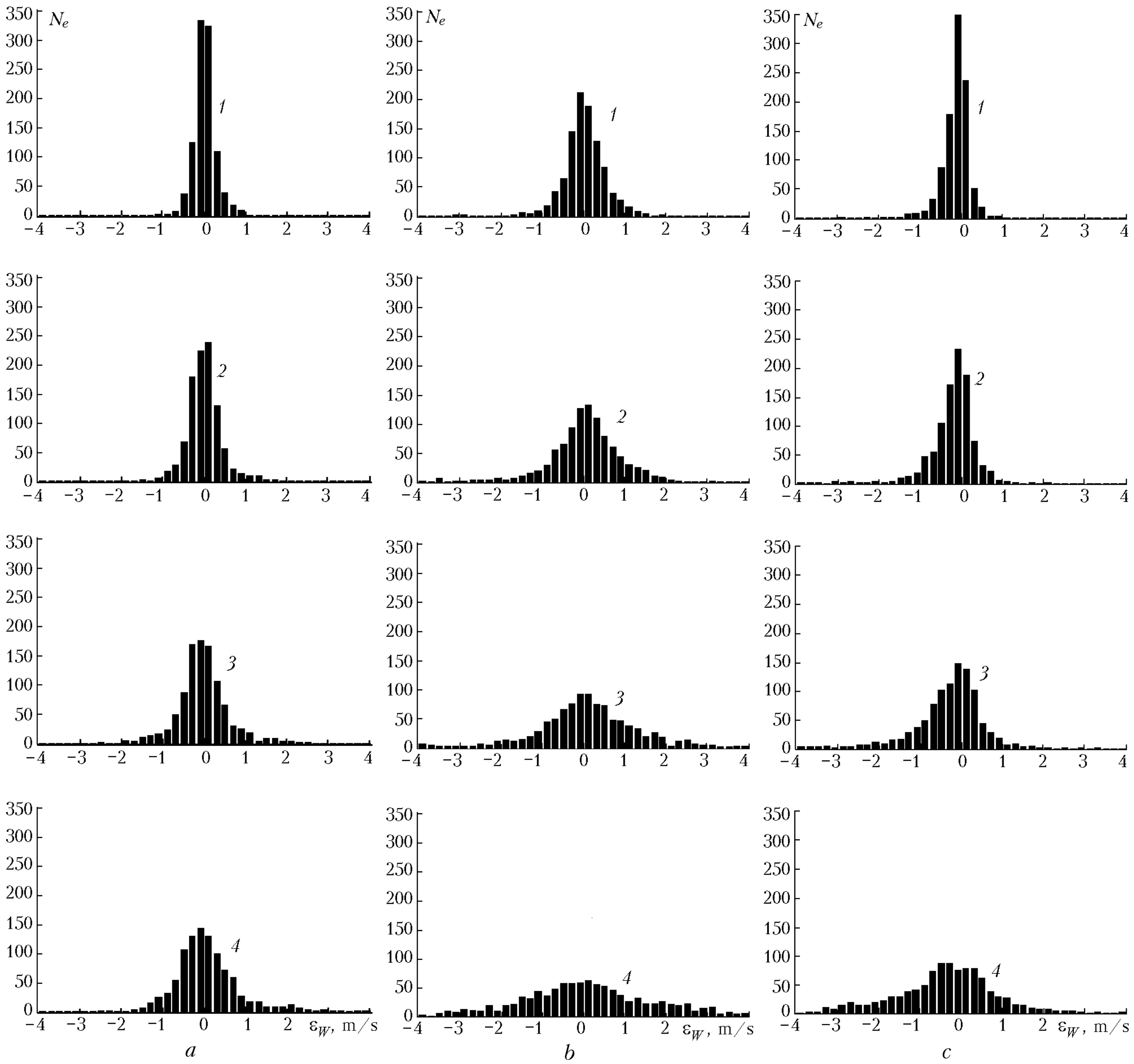


**Fig. 5.** Histograms of errors of estimating the Doppler broadening $\varepsilon_W$ at $n = 1$ and $SNR = 1$ (*a*); $n = 1$ and $SNR = 0.1$ (*b*); $n = 100$ and $SNR = 0.01$ (*c*); $\varepsilon = 10^{-3}$ (*1*); $5{\cdot}10^{-3}$ (*2*); $1.5{\cdot}10^{-2}$ (*3*), and $4.5{\cdot}10^{-2}$ m$^2$/s$^3$ (*4*).

By this it is meant that fluctuations of the Doppler spectral broadening $\Delta V_D$ caused by the large-scale wind inhomogeneities, result in a small random overlapping of the intervals determining the turbulence intensity in forces according to Table 2: $\{\sigma_s[1 - E_{\Delta V}]; \sigma_s[1 + E_{\Delta V}]\} = \{0.7\sigma_s; 1.3\sigma_s\}$ (in our case $\sigma_s \approx \sigma_{st}$). Hence, it follows that the error in determination of the intensity of clear sky turbulence will not be large even under conditions of strong sidewind.

## Conclusion

The study has been presented in this paper based on the numerical simulation made into the possibilities of sounding the clear sky turbulence with an airborne coherent Doppler lidar. The data on turbulence are extracted from the width of the lidar-return power spectrum estimated with the use of fitting procedure of the spectrum to the Gaussian dependence on the frequency (velocity).

From the numerical simulation it follows that the accuracy of turbulence estimating from lidar measurements depends on the turbulence intensity (the dissipation rate $\varepsilon$); the signal-to-noise ratio (*SNR*) and the order of spectral accumulation (the number of sounding pulses $n$). It is shown that from the measurements using a single sounding pulse ($n = 1$), it is possible to determine the turbulence level only at

*SNR* 0.1. In the case of $SNR = 0.01$ the spectra accumulation is needed, at least, from one hundred sounding pulses ($n = 100$).

## References

1. N.K. Vinnichenko, N.Z. Pinus, S.M. Shmeter, and T.N. Shur, *Turbulence in the Free Atmosphere* (Gidrometeoizdat, Leningrad, 1976), 287 pp.

2. S.M. Hannon, H.R. Badley, D.A. Bowdle, D.C. Soreide, R.K. Bogue, and L.J. Ehernberger, in: *Tenth Biennial Coherent Laser Radar Technology and Application Conference*, Oregon (1999), pp. 20–23.

3. V.A. Banakh and I.N. Smalikho, Atmos. Oceanic Opt. **10**, No. 12, 957–965 (1997).

4. R.G. Frehlich and M.J. Kavaya, Appl. Opt. **30**, No. 36, 5325–5352 (1991).

5. S.W. Henderson, S.M. Hannon and J.R. Magee, in: *Proc. 7th Conference on Coherent Laser Radar Applications and Technology* (Paris, France, 1993), pp. 169–173.

6. V.E. Zuev and G.M. Krekov, *Optical Models of the Atmosphere* (Gidrometeoizdat, Leningrad, 1986), 256 pp.